

A DUAL-MODE GYROSCOPE ARCHITECTURE WITH IN-RUN MODE-MATCHING CAPABILITY AND INHERENT BIAS CANCELLATION

A. Norouzpour-Shirazi¹, D.E. Serrano², M.F. Zaman², G. Casinovi¹, and F. Ayazi^{1,2}
¹Georgia Institute of Technology, Atlanta, GA, USA
²Qualtré Inc., Marlborough, MA, USA

ABSTRACT

This paper introduces a novel dual-mode actuation and sensing scheme for readout and calibration of axisymmetric Coriolis resonant gyroscopes. The proposed scheme actuates both gyroscope modes simultaneously with the same in-phase excitation, senses both modes concurrently, and utilizes the sum and difference of the sense signals to demonstrate complete cancellation of the gyroscope bias terms, and provide automatic in-run mode-matching capability. Moreover, the architecture provides twofold enhancement of angular rate sensitivity and signal-to-noise performance, as compared to conventional single-mode excitation of the same gyroscope. We demonstrate, for the first time 45× reduction in temperature drift of bias of a 2.6 MHz 650 μm diameter substrate-decoupled BAW gyroscope and a bias stability of 5.4 °/hr, paving the way towards near-zero-drift gyroscopes.

KEYWORDS

Dual-mode gyroscope, in-run bias calibration, automatic mode-matching, BAW gyroscope.

INTRODUCTION

The quest for zero-drift gyroscopes that can provide navigation functionality over long periods of time has led to extensive research on gyroscope bias and scale factor calibration techniques [1]-[3]. Bias calibration specifically is crucial to long term navigation applications.

The drift of the gyroscope bias can be mechanically attributed to the cross-stiffness and cross-damping coupling terms in the gyroscope equations. The long-term drift of the magnitude of these coupling terms with temperature and time, results in long-term drift of the gyroscope bias in a coherent demodulation interface scheme. Besides directly increasing the rate random walk (RRW) of the gyroscope, these coupling terms affect angle random walk (ARW) by down-converting additional noise from the drive loop oscillation signal. Therefore, an efficient gyroscope bias calibration scheme requires complete elimination of these coupling terms from the gyroscope electrical outputs, if not from the mechanical gyroscope itself. Fortunately, the magnitudes of the corresponding mechanical coupling terms are equal between the two modes. Therefore, an effective way of cancelling the bias errors is to use a differential architecture that excites two identical gyroscopic modes to cancel the common-mode bias terms and amplify the differential Coriolis component, in the same manner as a

differential amplifier.

Mode reversal [1] has been presented in the past as a technique to reduce drift in vibratory gyroscopes, by measuring the gyroscope bias in two consecutive phases and cancelling the bias data of each phase with that of the previous phase. Despite its effectiveness in cancelling the common-mode bias components, mode reversal suffers from system complexity and bandwidth limitation due to switching, while the switching rate itself is limited by the gyroscope settling time during each phase. Moreover, the switching may cause aliasing of uncorrelated high frequency rate and noise terms into the baseband.

Automatic in-run mode-matching is another necessary component of a self-calibration scheme in a mode-matched gyroscope system. In addition to providing maximum sensitivity and signal-to-noise performance [4], automatic mode-matching improves the stability of the gyroscope bias and scale factor by maintaining zero split between the two modes. The complicated techniques used in the past for in-run mode-matching [5], [6], do not provide a direct measure of mode split, but rather track the split variations by monitoring the amplitude or phase variations of the gyroscope outputs, which can be challenging in presence of temperature-induced errors in both gyroscope outputs and gain and phase of the circuits.

This paper presents for the first time, a dual-mode simultaneous actuation and sensing scheme for axisymmetric resonant gyroscopes. Both orthogonal degenerate modes of the gyroscope are actuated by the same excitation signal and sensed concurrently. Using the difference of the mode outputs, the identical common-mode bias errors cancel out each other to reduce the total bias error by close to an order of magnitude, while the opposite-phase Coriolis components add up to double the rate sensitivity and signal-to-noise ratio (SNR). Moreover, the difference signal provides a mode-split indicator that is used as a direct measure of mode split to enable efficient automatic in-run mode-matching of the gyroscope.

System Description

The schematic of the proposed system architecture is shown in Fig. 1. Degenerate elliptical modes ($m = 3$) of a substrate decoupled (SD) bulk acoustic wave (BAW) gyroscope [7] are both actuated and sensed simultaneously. The sum of the two sense outputs is used for self-sustaining closed-loop actuation of the gyroscope. The difference of the sense outputs is multiplied by the drive actuation signal for coherent rate demodulation from the Coriolis signal.

The following set of equations can be solved to find the

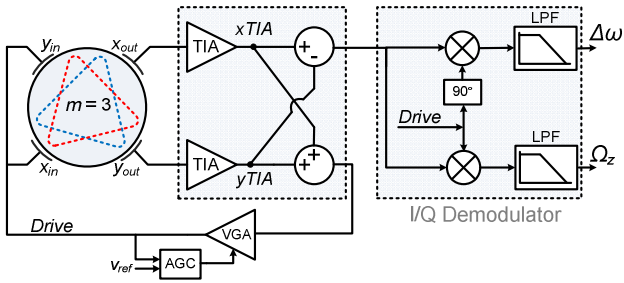


Figure 1: Proposed gyroscope architecture; both $m=3$ modes of the 2.6-MHz BAW gyroscope are actuated and sensed simultaneously. The difference output is used for rate detection and summation is used to close the drive loop.

gyroscope response to dual-mode in-phase actuation

$$\begin{aligned} m\ddot{x} + d_{xx}\dot{x} + k_{xx}x + k_{yx}y + d_{yx}\dot{y} &= f_x(t) - 2m\lambda\Omega_z\dot{y} \\ m\ddot{y} + d_{yy}\dot{y} + k_{yy}y + k_{xy}x + d_{xy}\dot{x} &= f_y(t) + 2m\lambda\Omega_z\dot{x} \end{aligned} \quad (1)$$

The displacement and velocity of each resonance mode with $\omega_i = \sqrt{k_{ii}/m}$, and $Q = m\omega_i/d_{ii}$ can be calculated based on the above equations, for given values of rotation Ω_z , angular gain λ , and mode coupling coefficients k_{xy} , k_{yx} , d_{xy} , and d_{yx} .

In the dual-mode actuation scheme, assuming that both gyroscope modes are actuated at $\omega_0 = (\omega_x + \omega_y)/2$, with identical forces $f_x(t) = f_y(t) = f_0 \cos \omega_0 t$, the displacement phasor response of the sum and difference of the modes are

$$\begin{aligned} X_{Sum}(j\omega_0) &= \frac{\left(\frac{2F_0}{m\omega_0}\right) \left[\frac{(\Delta\omega)^2}{4\omega_0} + j\frac{\omega_0}{Q} - \frac{\omega_{xy}^2}{\omega_0} - j\frac{\omega_{xy}}{Q_{xy}} \right]}{\left[-\left((\Delta\omega)^2 + \left(\frac{\omega_0}{Q}\right)^2 + 4\lambda^2\Omega_z^2 \right) + \left(\frac{\omega_{xy}^4}{\omega_0^2} - \frac{\omega_{xy}^2}{Q_{xy}^2} \right) + j\left(\frac{(\Delta\omega)^2}{2Q} + \frac{2\omega_{xy}^2}{\omega_0} \frac{\omega_{xy}}{Q_{xy}} \right) \right]} \\ X_{Diff}(j\omega_0) &= \frac{\left(\frac{2F_0}{m\omega_0}\right) \left[\Delta\omega + \frac{\Delta\omega}{2Q} + j2\lambda\Omega_z \right]}{\left[-\left((\Delta\omega)^2 + \left(\frac{\omega_0}{Q}\right)^2 + 4\lambda^2\Omega_z^2 \right) + \left(\frac{\omega_{xy}^4}{\omega_0^2} - \frac{\omega_{xy}^2}{Q_{xy}^2} \right) + j\left(\frac{(\Delta\omega)^2}{2Q} + \frac{2\omega_{xy}^2}{\omega_0} \frac{\omega_{xy}}{Q_{xy}} \right) \right]} \end{aligned} \quad (2)$$

where k_{xy}/m and d_{xy}/m translate to ω_{xy}^2 and ω_{xy}/Q_{xy} , respectively, and $\Delta\omega = \omega_y - \omega_x$. In the numerator of the difference output, the common-mode coupling terms in the x - and y - sense outputs are completely cancelled out, unlike in conventional single-axis actuation where the numerator would contain both Coriolis and coupling terms. Moreover, the differential Coriolis terms in the two sense outputs add and thus double the angular rate sensitivity. In theory, the added sensitivity results in two times enhancement of SNR, since the noises of the two sense outputs are uncorrelated.

The bias components in the denominator of both sum, X_{Sum} , and difference, X_{Diff} , can cause residual bias errors.

The effect of these errors is reduced by using high frequency and high bandwidth gyroscopes in which these errors become negligible compared to the ω_0/Q term.

By cancelling out the bias components from X_{Diff} , the proposed scheme can effectively improve the bias stability of the gyroscope. Furthermore, the bias cancellation can significantly reduce the RRW and effectively compensate the temperature drift of the sensor bias. The reduction of the zero-rate output (ZRO) errors also enhances the dynamic range of the electronics by allowing higher front-end gain.

It can be shown that in dual-mode actuation, the individual modes contain opposite-phase Coriolis terms, making them not suitable for closed-loop actuation. The significance of summing the outputs is in the Coriolis cancellation that it provides for rate-independent actuation. Moreover, it can be shown that with a split of $\Delta\omega$ between the mode frequencies, a series-mode oscillator loop operating based on the sum output, locks into the midpoint of the two frequencies, i.e. $\omega_0 = (\omega_x + \omega_y)/2$, which validates the assumption made for derivation of (2) and (3).

In a simplified model, neglecting the bias terms corresponding to ω_{xy}^2 and ω_{xy}/Q_{xy} compared to the relatively large ω_0/Q term in a high bandwidth gyroscope, and given that $\Delta\omega \ll \omega_0$, X_{Sum} and X_{Diff} can be rewritten as

$$\begin{aligned} X_{Sum}(j\omega_0) &\approx -\frac{2F_0}{m\omega_0} \frac{j\frac{\omega_0}{Q}}{(\Delta\omega)^2 + \left(\frac{\omega_0}{Q}\right)^2 + 4\lambda^2\Omega_z^2} \\ X_{Diff}(j\omega_0) &\approx -\frac{2F_0}{m\omega_0} \frac{\Delta\omega + j2\lambda\Omega_z}{(\Delta\omega)^2 + \left(\frac{\omega_0}{Q}\right)^2 + 4\lambda^2\Omega_z^2} \end{aligned} \quad (3)$$

A unique feature of the proposed scheme is the rate- and bias-independent frequency split indicator provided by the quadrature-phase component of the difference output current. The quadrature-phase relationship of this split indicator with the rate output enables real-time monitoring of mode split during the gyroscope operation, assuming the gyroscope operation is initialized at near mode-matched condition. Therefore, it enables in-run automatic mode-matching, even in presence of mechanical rotation, which has been challenging in single-mode gyroscopes [5], [6].

The bias cancellation together with automatic mode-matching capability provided by the dual-mode architecture can reduce gyroscope drift significantly, and thus enable near-zero-drift gyroscope, as shown by the experimental results presented in the next section.

Experimental Results

The proposed architecture has been implemented on a PCB prototype to interface with a 2.6 MHz SD BAW gyroscope with a Q of 37,000 for each $m=3$ mode. Figure 2a shows the mode shapes of the BAW gyroscope. A SEM picture of the 650- μm -diameter BAW gyroscope is shown in Fig. 2b, and Fig. 3b shows the photograph of the wafer-level packaged $2 \times 2 \times 0.9 \text{ mm}^3$ gyroscope die.

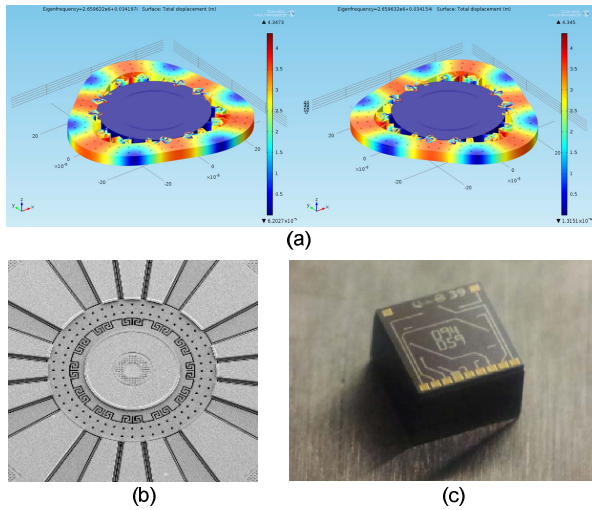


Figure 2: (a) $m=3$ mode shapes of the SD BAW gyroscope, (b) SEM picture of the 650- μm -diameter BAW gyroscope, (c) die photograph of the $2 \times 2 \times 0.9 \text{ mm}^3$ wafer-level packaged BAW gyroscope.

The gyroscope die is mounted on the PCB together with actuation and readout circuits. An HF2LI lock-in amplifier provides closed-loop actuation, rate demodulation, and in-run automatic mode-matching, while the transimpedance amplifiers (TIA), summation and difference functions, and actuation amplifiers are implemented with analog discrete electronics on the PCB. For the TIAs, OPA657 (TI) has been used, while the other functions are implemented with AD8058 dual amplifiers (ADI). The measured results are compared to conventional single-mode actuation using the same gyroscope by reconfiguring the interface electronics.

Figure 3 shows the frequency response of the gyroscope modes when only the x -mode is actuated and both x - and y -modes are sensed, and also the response of the summation and difference outputs when both modes are simultaneously actuated and sensed. As expected from theory, the dual-mode summation output shows 6dB higher gain than the x -mode output in single-mode actuation. With dual-mode actuation, the difference output shows 24dB lower ZRO than the y -mode output in single-mode actuation.

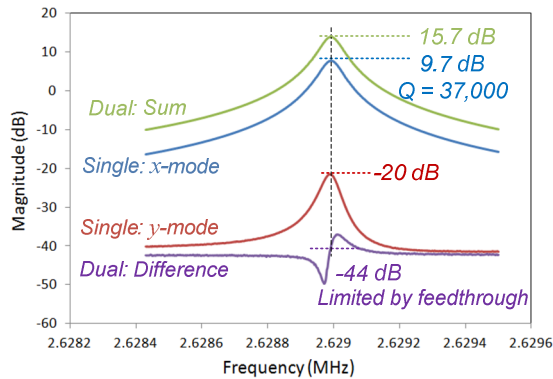


Figure 3: Open-loop response of the difference output in dual-mode gyroscope shows 24dB lower ZRO than sense-mode quadrature in single-mode AM scheme.

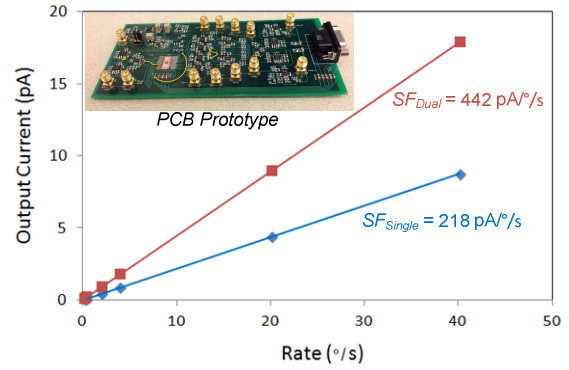


Figure 4: Measured sensitivity of the dual-mode architecture is twice larger than the sensitivity of coherent demodulation using the same gyroscope. Inset shows PCB prototype with the MEMS die mounted on it.

Figure 4 shows twofold increase in the angular rate sensitivity. The rate sensitivity of both architectures is characterized at rotation rates in a range of 1-40 $^\circ/\text{s}$, where the single-mode and dual-mode actuation schemes show scale factor values of 218 $\text{pA}/^\circ/\text{s}$ and 442 $\text{pA}/^\circ/\text{s}$, respectively. The inset shows the PCB prototype with the MEMS die mounted on it.

Both single-mode and dual-mode actuation schemes were characterized for bias stability. Figure 5 shows the Allan variance plot for both architectures, measured at room temperature. The dual-mode actuation scheme improves the bias drift of the BAW gyroscope from 25.6 $^\circ/\text{hr}$ at 10 sec averaging time in conventional scheme to as low as 5.4 $^\circ/\text{hr}$ at 600 sec averaging time. The 60x improvement in averaging time makes this scheme more suitable for long-term navigation. Moreover, the dual-mode architecture consistently improves ARW from 1 $^\circ/\sqrt{\text{hr}}$ to 0.7 $^\circ/\sqrt{\text{hr}}$, due to the 3-dB SNR enhancement.

In another set of measurements, the two schemes were characterized for temperature stability of output bias. Utilizing the mode split indicator in the quadrature-phase

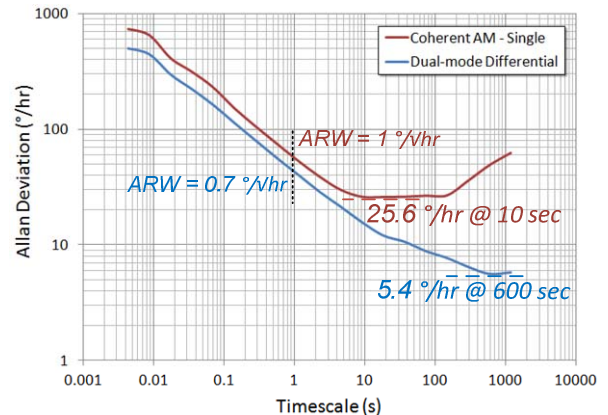


Figure 5: Allan deviation plots for both architectures; Dual-mode architecture improves the bias drift of the gyroscope by almost 5-times from 25.6 $^\circ/\text{hr}$ at 10 sec, to as low as 5.4 $^\circ/\text{hr}$ at 600 sec. The ARW is consistently improved by 1.4 times, attributed to 3-dB SNR improvement.

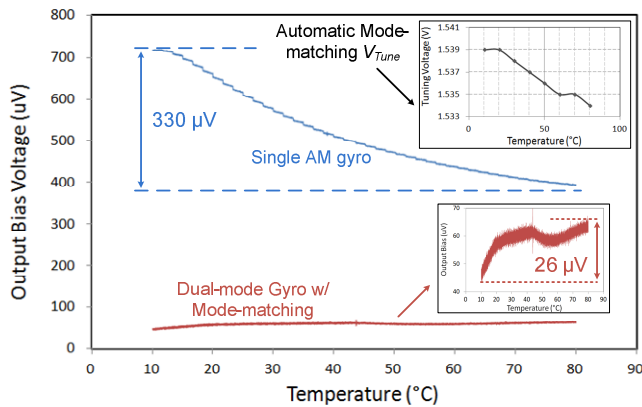


Figure 6: Bias cancellation reduces the temperature drift of bias from $330 \mu\text{V}$ in coherent demodulation to $26 \mu\text{V}$ in dual-mode architecture, across a $10\text{-}80 \text{ }^\circ\text{C}$ temperature range. Automatic mode-matching is implemented to improve stability over temperature.

component of the difference output, an in-run automatic mode-matching control loop was implemented. A PID controller in the lock-in amplifier controls the tuning voltage of the x -mode, V_{Tx} , to keep the mode split indicator at 0 V , thereby maintaining mode-matched condition at all temperatures. Figure 6 compares the temperature drift of the gyroscope bias voltage in the two architectures. The bias cancellation technique together with automatic mode-matching, reduce the overall drift of bias voltage from $330 \mu\text{V}$ to $26 \mu\text{V}$ across a $10\text{-}80 \text{ }^\circ\text{C}$ temperature range. The top right inset shows the tuning voltage generated by the PID controller to maintain mode-matched condition.

Figure 7 compares the bias drift equivalent input rotation in $^\circ/\text{s}$ for both configurations, demonstrating for the first time $45\times$ reduction in the overall drift of the bias, down to $3 \text{ }^\circ/\text{s}$, over the entire temperature range.

CONCLUSIONS

A dual-mode actuation and sensing scheme was introduced in this paper. Both orthogonal degenerate modes of an axisymmetric BAW gyroscope are actuated and sensed simultaneously. The sum of the two mode outputs is used to cancel the effect of rate on the self-sustaining drive loop for rate-independent actuation of the gyroscope, and the difference of the two mode outputs is used for rate demodulation. Due to the equality of the mode coupling terms in the gyroscope equation, these terms are almost eliminated from the difference output, which improves the bias drift performance and enhances the overall dynamic range of the gyroscope system. Moreover, the architecture increases the gyroscope rate sensitivity by twice, which theoretically enhances the SNR and ARW by two times.

A unique feature of the proposed system is the mode split indicator signal provided by the quadrature-phase component of the difference output current. The indicator was used to provide in-run automatic mode-matching for the gyroscope. The bias cancellation scheme together with the automatic mode-matching are capable of reducing the drift

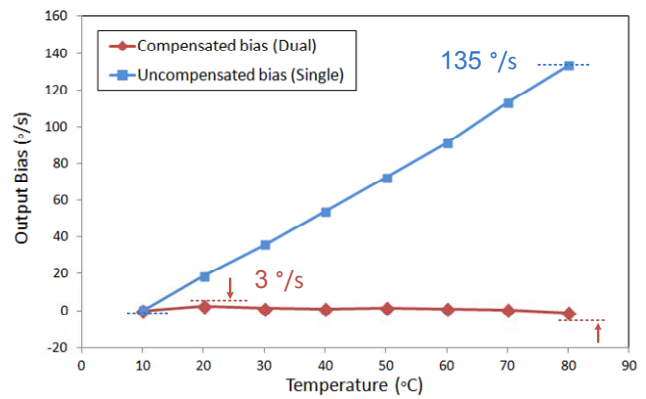


Figure 7: The bias cancellation reduces the temperature drift of gyroscope bias from $135 \text{ }^\circ/\text{s}$ in single-mode AM gyro down to $3 \text{ }^\circ/\text{s}$ in dual-mode architecture, across the $10\text{-}80\text{ }^\circ\text{C}$ temperature range.

of the gyroscope bias by 45 times, from $135 \text{ }^\circ/\text{s}$ to only $3 \text{ }^\circ/\text{s}$ over a relatively large temperature range of $10\text{-}80 \text{ }^\circ\text{C}$, paving the way towards near-zero-drift MEMS gyroscopes.

ACKNOWLEDGEMENTS

The authors wish to thank DARPA for supporting this work under the PASCAL program, contract #W31P4Q-12-1-0004. The authors would like to also thank Mojtaba Hodjat-Shamami for helpful discussions.

REFERENCES

- [1] David M. Rozelle, "Self calibrating gyroscope system," U.S. Patent No. 7,912,664, Mar 22, 2011.
- [2] A. N. Shirazi, et al, "Combined phase-readout and self-calibration of MEMS gyroscopes," *Solid-State Sensors, Actuators and Microsystems, 2013 Transducers & Eurosensors XXVII: The 17th International Conference on*, pp.960-963, 16-20 June 2013.
- [3] I.P. Prikhodko et al, "In-run bias self-calibration for low-cost MEMS vibratory gyroscopes," *PLANS 2014*, pp.515-518, 5-8 May 2014.
- [4] F. Ayazi, "Multi-DOF inertial MEMS: From gaming to dead reckoning," *Solid-State Sensors, Actuators and Microsystems Conference (TRANSDUCERS)*, 2011 16th International, pp.2805-2808, 5-9 June 2011.
- [5] R. Antonello, et al, "Automatic Mode Matching in MEMS Vibrating Gyroscopes Using Extremum-Seeking Control," *Industrial Electronics, IEEE Transactions on*, vol.56, no.10, pp.3880-3891, 2009.
- [6] S. Sung, et al, "On the Mode-Matched control of MEMS vibratory gyroscope via Phase-Domain analysis and design," *IEEE/ASME Transactions on Mechatronics*, vol. 14, no. 4, pp. 446-455, Aug. 2009.
- [7] D.E. Serrano, "Integrated Inertial Measurement Units Using Silicon Bulk-Acoustic Wave Gyroscopes," Ph.D. Dissertation, Georgia Institute of Technology, 2014.

CONTACT

*A. N. Shirazi, tel: +1-404-385-6693; arashk.n@gatech.edu